

# The impact of peculiar velocities on supernova cosmology

Roya Mohayaee<sup>1</sup>, Mohamed Rameez<sup>2</sup>, and Subir Sarkar<sup>3</sup>

<sup>1</sup> CNRS, UPMC, Institut d'Astrophysique de Paris, 98 bis Bld Arago, Paris, France

<sup>2</sup> Tata Institute of Fundamental Research, Homi Bhabha Road, Mumbai 400005, India

<sup>3</sup> Rudolf Peierls Centre for Theoretical Physics, University of Oxford, Parks Road, Oxford OX1 3PU, United Kingdom

## ABSTRACT

**Context.** We study correlated fluctuations of Type Ia supernova observables due to peculiar velocities of both the observer and the supernova host galaxies, and their impact on cosmological parameter estimation.

**Aims.** We aim to demonstrate using the CosmicFlows-3 dataset that at low redshifts the corrections for peculiar velocities in the JLA catalogue have been systematically underestimated.

**Methods.** By querying a horizon-size N-body simulation we find that compared to a randomly placed observer, an observer in an environment like our local Universe will see 2–8 times stronger correlations between supernovae in the JLA catalogue. Hence the covariances usually employed underestimate the effects of coherent motion of the supernova host galaxies.

**Results.** Contrary to previous studies which asserted that peculiar velocities have negligible effect on cosmological parameter estimation, we find that when such correlations are taken into account the JLA data favour significantly smaller values of the dark energy density than in the standard  $\Lambda$ CDM model. A joint fit to simultaneously determine the cosmological parameters and the bulk flow indicates that the latter is around  $250 \text{ km s}^{-1}$  even beyond  $200h^{-1} \text{ Mpc}$ .

**Conclusions.** The local bulk flow is thus an essential nuisance parameter to be included in analyses of the supernova Hubble diagram.

**Key words.** cosmology:observations – cosmological parameters – large-scale structure of universe – cosmology:theory

## 1. Introduction

Type Ia supernovae (SNe Ia) have been observed out to redshifts  $z \gtrsim 1$  and are considered to be ‘standardisable candles’ on the basis of empirical correlations that are observed between the peak magnitude and the light-curve width (see, Leibundgut 2000). Using these as distance indicators it was famously inferred that the Hubble expansion rate is presently accelerating (Perlmutter et al. 1999; Riess et al. 1998) — leading to today’s standard  $\Lambda$ CDM model which is dominated by a Cosmological Constant (aka dark energy) with  $\Omega_\Lambda \simeq 0.7$  and  $\Omega_m \simeq 0.3$ .

However, to obtain the cosmological redshift from the value measured from Earth corrections have to be made for ‘peculiar’ (non-Hubble) velocities. These are typically a few hundreds of  $\text{km s}^{-1}$ , so would appear to only be relevant at low redshift  $z \lesssim 0.1$ , since the expansion rate is  $h \equiv H_0/100 \text{ Km s}^{-1} \text{ Mpc}^{-1} \simeq 0.7$ . Even so they can affect the analysis at high redshift too if proper care is not taken. Various methods for accounting for peculiar velocities have been proposed (Hudson et al. 2004); it is a difficult task as there are just a few available measurements. Hence this problem has often just been circumvented by simply excluding from cosmological fits all the SNe Ia at low redshifts. However this severely deprecates the sample statistics (since about half of all known SNe Ia are in fact local) and moreover it is somewhat arbitrary, *e.g.* cuts have been applied at both  $z = 0.01$  and at  $z = 0.025$  (Conley et al. 2011). Another option is to allow for an *uncorrelated*, and again somewhat arbitrary, dispersion in the velocities of SNe Ia, *e.g.* Perlmutter et al. (1999) took the redshift uncertainty due to peculiar velocities to be  $c\sigma_z = 300 \text{ km s}^{-1}$ , while Riess et al. (1998) used  $c\sigma_z = 200 \text{ km s}^{-1}$ .

The alternative is to *correct* for the peculiar velocities (Neill et al. 2007): for this purpose the IRAS PSCZ catalogue (Saunders et al. 2000), the SMAC catalogue of clusters (Hudson et al. 2004) and the 2M++ catalogue (Carrick et al. 2015) have been used to infer the peculiar velocity field from the underlying density field. However these catalogues are rather limited and can be biased, moreover linear perturbation theory is used, hence the extracted velocities are somewhat uncertain. Furthermore, these analyses assume convergence to the cosmic rest frame at  $\gtrsim 100h^{-1} \text{ Mpc}$ , as is expected in the framework of the standard  $\Lambda$ CDM model, even though this is contradicted by observations (Hudson et al. 2004; Watkins et al. 2009; Lavaux et al. 2010; Colin et al. 2011; Feindt et al. 2013; Magoulas et al. 2016). It is in any case inappropriate to use  $\Lambda$ CDM to make such corrections since the model is itself a subject of the test being carried out.

Specifically in analyses of the SDSS-II/SNLS3 Joint Lightcurve Analysis (JLA) catalogue of 740 SNe Ia (Betoule et al. 2014), and the subsequent Pantheon catalogue of 1048 SNe Ia (which includes 279 SNe Ia from Pan-STARRS1) (Scolnic et al. 2017), the low redshift SNe Ia have been retained in the cosmological fits by thus ‘correcting’ the individual redshifts and magnitudes of the SNe for the local ‘bulk flow’ inferred from density field surveys out to  $z \sim 0.04$  (Hudson et al. 2004) and  $z \sim 0.067$  (Carrick et al. 2015). However as noted by Colin et al. (2019a), in both analyses SNe Ia immediately outside the survey volume of the peculiar velocity field were arbitrarily assumed to be at rest with respect to the cosmic rest frame, despite the fact that these very surveys detected a bulk flow extending *beyond* the survey volume of  $372 \pm 127 \text{ km s}^{-1}$  and  $159 \pm 23 \text{ km s}^{-1}$ , respectively. Moreover the JLA and Pantheon analyses adopted

different values of  $150 \text{ km s}^{-1}$  and  $250 \text{ km s}^{-1}$  respectively for the dispersion  $c\sigma_z$  of the bulk flow velocity.

On the theoretical side, the *correlated* fluctuations of SNe Ia magnitudes due to peculiar velocities as well as the impact on cosmological parameter estimation of making such corrections have been studied by Hui & Greene (2006); Neill et al. (2007); Davis et al. (2011); Huterer et al. (2015), however all these studies assumed that the peculiar velocity statistics are those expected around a *typical* observer in a  $\Lambda$ CDM universe. Such an observer should in fact not observe a bulk flow exceeding  $200 \text{ km s}^{-1}$  beyond  $100 h^{-1} \text{ Mpc}$  ( $\Rightarrow z \approx 0.033$ ), independently of the form of the matter power spectrum (see, e.g., Hunt & Sarkar 2010), so clearly this assumption is in tension with reality.

Moreover the peculiar velocity corrections applied to both JLA and Pantheon contain significant errors and inconsistencies (Colin et al. 2019a; Rameez & Sarkar 2021). Since the covariance matrices for peculiar velocity corrections have not been provided separately, the impact of these errors on cosmological parameter estimation cannot be quantified.

Recent observations of bulk flows suggest that we are *not* a typical (or ‘Copernican’) observer in a  $\Lambda$ CDM universe (Hellwing et al. 2017, 2018; Rameez et al. 2018). We discuss here the correlated fluctuations of SNe Ia magnitudes and redshifts due to the peculiar velocities and bulk flows in and around ‘Local Universe (LU)-like’ environments in the  $z = 0$  halo catalogue of the DarkSky  $\Lambda$ CDM simulations (Skillman et al. 2014). We find that previous theoretical predictions for randomly selected typical observers (Hui & Greene 2006) have *underestimated* the actual covariances for observers like ourselves by a factor of 2–8.

We discuss (§ 2) the peculiar velocity corrections employed in JLA (Betoule et al. 2014) and show that these are both arbitrary and incomplete (§ 3). We compare the magnitude of the velocities used for the corrections in JLA against those obtained from the CosmicFlows-3 (CF3) compilation (Tully et al. 2016) and demonstrate that the JLA values are *underestimates* by 48% on average. We also review the various relevant sources of uncertainties and dispersions that go into the JLA cosmological fits. We then explore (§ 4) various methods to fit for the extent of the bulk flow in the LU and present our likelihood analysis (§ 5). This is followed by a discussion of related work (§ 6). An Appendix presents the standard methodology of cosmology with supernovae (§ A), and the JLA catalogue (§ B).

We find that for any consistent treatment of the peculiar velocities (including ignoring them altogether), the JLA dataset favours  $\Omega_\Lambda \lesssim 0.4$  and is consistent with a non-accelerating Universe at  $< 2\sigma$ . Larger values of  $\Omega_\Lambda$  which have been found in other analyses of the JLA catalogue (Nielsen et al. 2016; Rubin & Hayden 2016) are in fact due to the incomplete peculiar velocity ‘corrections’ applied. We demonstrate that the data favour a fast ( $> 250 \text{ km s}^{-1}$ ) bulk flow extending out to  $> 200 h^{-1} \text{ Mpc}$ , which is quite unexpected in the standard  $\Lambda$ CDM model.

## 2. Peculiar Velocities and SNe Ia observables

Assuming that the CMB dipole is entirely due to our motion wrt the cosmic rest frame (‘CMB frame’) in which the universe looks isotropic, (and the luminosity distance  $d_L$  is related to the redshift  $z$  as in eq.A.2), the redshift of a supernova in the heliocentric frame  $z_{\text{hel}}$  (after correcting the actually measured redshift for the Earth’s motion around the Sun) is related to its redshift  $z$  in the CMB frame (sometimes labelled  $z_{\text{CMB}}$ ) as:

$$1 + z_{\text{hel}} = (1 + z_\odot) \times (1 + z_{\text{SN}}) \times (1 + z), \quad (1)$$

where  $z_\odot$  is the redshift induced by our motion w.r.t. the CMB and  $z_{\text{SN}}$  is the redshift due to the peculiar motion of supernova host galaxy in the CMB frame. The luminosity distance is similarly corrected as:

$$d_L(z_{\text{hel}}) = d_L(z)(1 + z_\odot) \times (1 + z_{\text{SN}})^2 \quad (2)$$

to obtain the  $d_L$  as a function of  $z$  for the standard  $\Lambda$ CDM model (see § A). The covariance of SNe Ia magnitudes due to peculiar velocities is then given by (Hui & Greene 2006; Davis et al. 2011; Huterer et al. 2015):

$$S_{ij} = \langle \delta m_i \delta m_j \rangle = \left[ \frac{5}{\ln 10} \right]^2 \frac{(1 + z_i)^2}{H(z_i) d_L(z_i)} \frac{(1 + z_j)^2}{H(z_j) d_L(z_j)} \xi_{ij}, \quad (3)$$

where

$$\xi_{ij} = \langle (\mathbf{v}_i \cdot \hat{\mathbf{n}}_i)(\mathbf{v}_j \cdot \hat{\mathbf{n}}_j) \rangle = \frac{dD_i}{d\tau} \frac{dD_j}{d\tau} \int \frac{dk}{2\pi^2} P(k, a=1) \times \sum_l (2l+1) j'_l(k\chi_i) j'_l(k\chi_j) P_l(\hat{\mathbf{n}}_i \cdot \hat{\mathbf{n}}_j). \quad (4)$$

Here  $D_i$  is the linear structure growth factor at the redshift of the  $i^{\text{th}}$  SNe,  $j'_l$  is the derivative of the  $l^{\text{th}}$  spherical Bessel function and  $P_l$  is the Legendre polynomial of order  $l$ . Note that according to this expression the covariance in magnitudes between two SNe depends only on their relative angular separation (which comes in through  $P_l$ ) and is independent of their absolute directions.

N-body simulations can be used to estimate  $\xi_{ij}$  (eq.3) for different assumed observers. Fig. 1 compares  $S_{ij}$  evaluated using the  $\Lambda$ CDM expectation for  $\xi_{ij}$  with that read off the  $z = 0$  snapshot halo catalogue of the Dark Sky simulation, a Hubble volume, trillion-particle simulation (Skillman et al. 2014), for two very different classes of observers. For the ‘Copernican observer’ in Fig.1 (left), the halo containing the observer and its orientation are selected at random — such an observer sees the universe as isotropic and homogeneous. However for the constrained ‘LU-like observer’ (right), only halos satisfying the following criteria are considered (the first three being similar to those in Hellwing et al. (2017)):

- (i) The observer halo has a Milky Way (MW)-like mass, in the range  $2.2 \times 10^{11} < M_{200} < 1.4 \times 10^{12} M_\odot$  (Cautun et al. 2014) for the halo mass contained within 200 kpc.
- (ii) The bulk velocity in a sphere of  $R = 3.125 h^{-1} \text{ Mpc}$  centred on the observer is  $V = 622 \pm 150 \text{ km s}^{-1}$
- (iii) A Virgo-cluster like halo of mass  $M = (1.2 \pm 0.6) \times 10^{15} h^{-1} M_\odot$  is present at a distance  $D = 12 \pm 4 h^{-1} \text{ Mpc}$  from the observer.
- (iv) The angle between the bulk flow of (ii) and the direction to the Virgo-like halo of (iii) is  $(44.5 \pm 5)^\circ$ .
- (v) The bulk velocity in a sphere of  $R = 200 h^{-1} \text{ Mpc}$  centred on the observer is  $260 \pm 100 \text{ km s}^{-1}$  (Colin et al. 2011).
- (vi) The angle between the bulk flow of (v) and the direction to the Virgo-like halo of (iii) is  $(69.9 \pm 7.5)^\circ$ .
- (vii) The angle between the bulk flows of (ii) and (v) is  $(35.6 \pm 7.5)^\circ$ .

After an observer satisfying the above criteria is found, the entire system is rotated so that the direction of the bulk flow of criterion (ii) and the direction to the Virgo-like halo of criterion (iii) correspond to the real observed directions. The criterion on the bulk flow direction is exact, while the criterion on the direction to the Virgolike halo is imposed only on the azimuthal angle in a coordinate system in which the  $z$ -axis points towards

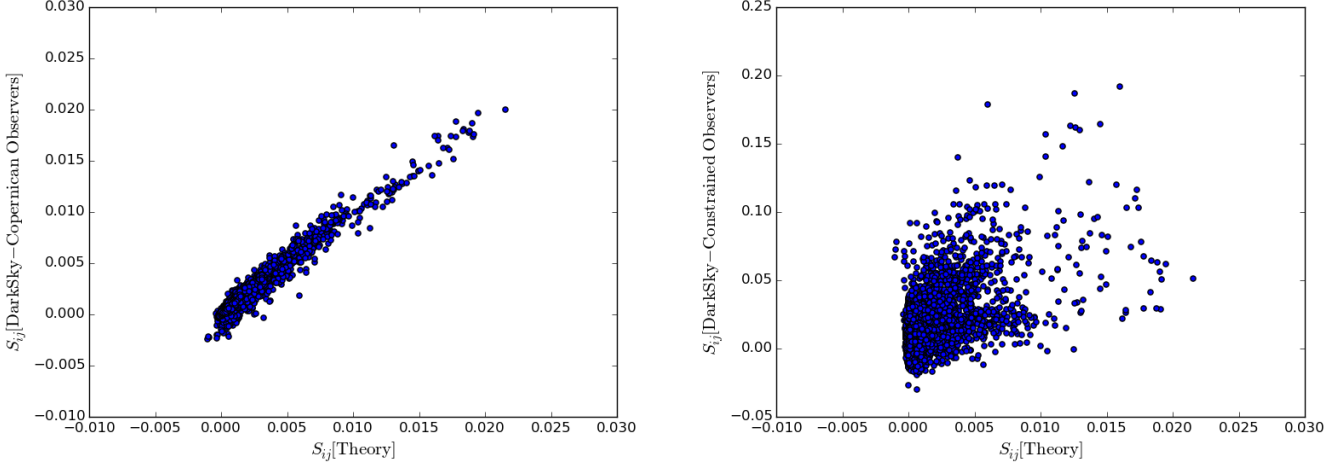


**Fig. 1.** The theoretically expected covariance  $S_{ij}$  (eq.3) plotted against the value found in N-body simulations — in regions around typical observers (left) and constrained ‘Local Universe-like’ observers (right). Each point is an average over 1000 observers.

the bulk flow direction. Criterion (iv) then suffices to orient the system. Note that the angular tolerances in (iv), (vi) and (vii) are not as stringent than current observational constraints, in order to limit the required computation time.

Subsequently, halos around the observer closest to the 3D coordinates of each JLA supernova are identified, and their velocities are queried. From these velocities,  $\xi_{ij}$  can be calculated. For the typical observer of Fig. 1 (left), none of the steps regarding directional orientation discussed above are considered and observers are simply picked at random. As seen in Fig. 1 (right), a realistic LU-like observer on average sees correlations 2-8 times *stronger* between the supernovae of a JLA like catalogue than does a typical observer, while the theoretical covariances of eq.(4) are valid only for idealised observers who see neither a local bulk flow nor a preferred orientation in the sky.

### 3. Peculiar velocity corrections in JLA

Colin et al. (2019a) pointed out that the peculiar velocity ‘corrections’ applied to the SNe Ia redshifts and magnitudes in the JLA catalogue (see § B) are neither consistent nor complete. SNe Ia immediately beyond  $z \sim 0.06$  are taken to be stationary w.r.t. the CMB and assumed to only have an uncorrelated velocity dispersion  $c\sigma_z = 150 \text{ km s}^{-1}$  in the cosmological fits, even though observations of clusters indicate a bulk velocity of  $372 \pm 127 \text{ km s}^{-1}$  due to sources beyond  $200h^{-1} \text{ Mpc}$  (Hudson et al. 2004). Unlike the intrinsic dispersion  $\sigma_{M_0}$  which is assumed to be redshift *independent*, the dispersion in the magnitudes as a result of the velocity dispersion is  $5\sigma_z/(z\log 10)$  i.e. the magnitudes of lower redshift supernovae are selectively more dispersed. As seen in Fig.2, the typical bulk flow in a  $\Lambda$ CDM universe (see, e.g. Hong et al. 2014) continues to much larger distances, with the velocity decreasing gradually. In some environments, the bulk velocity may even *increase* beyond a certain scale.

The CosmicFlows-3 (CF3) (Tully et al. 2016) compilation presents actual measurements of the peculiar velocities of 17,669 nearby galaxies, using various *independent* distance estimators such as the Tully-Fisher relationship. In Fig.3, we compare the velocities that have been used to correct the JLA redshifts with the velocities obtained from the CosmicFlows-3 compilation. The galaxy in the CF3 dataset corresponding to a JLA supernova is identified by cross-matching with a tolerance of  $0.01^0$ ,

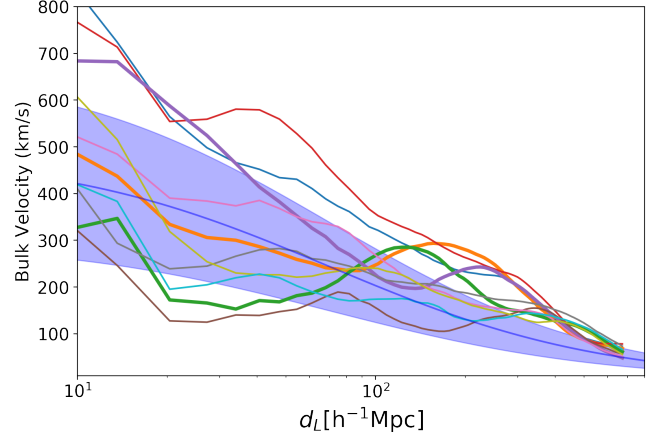


**Fig. 2.** The bulk flow velocity profiles around 10 random ‘local Universe-like’ observers satisfying the criteria in § 2. Note that the velocity profile around an individual observer need not decrease monotonically, even though the ensemble average in the  $\Lambda$ CDM model (dark blue curve) does so. The shaded blue region is the  $\pm 1\sigma$  band around the mean value.

using the tool *k3match*; Out of 119 JLA SNe Ia at  $z_{\text{cmb}} < 0.06$ , 112 have CF3 counterparts within  $0.01^0$ . It is seen from the regression line (Boggs et al. 1990) in Fig.3 that peculiar velocities have been systematically *underestimated* by 48% in the corrections applied in the JLA analysis (Betoule et al. 2014), compared to the actual measurements by CF3.

### 4. Fitting for a bulk flow

We consider two illustrative profiles for the bulk flow velocity: an exponentially falling one,

$$\langle v \rangle = P e^{-d_L/Q}, \quad (5)$$

where  $Q$  is the scale of the flow, and a linearly falling one,

$$\langle v \rangle = P - Q' d_L, \quad (6)$$

where  $Q'$  is a (dimensionless) scale parameter. In the latter parametrisation we ensure that the velocity never goes negative

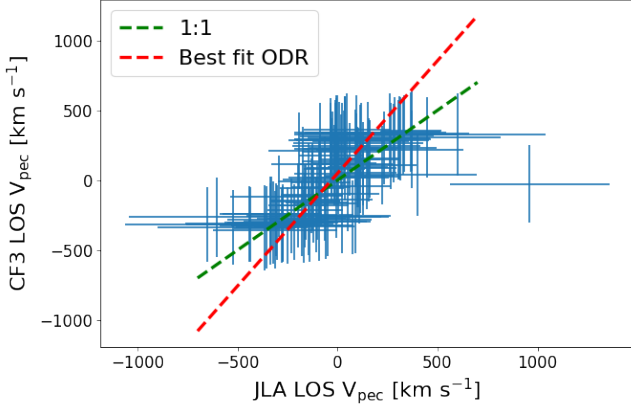


**Fig. 3.** The line-of-sight velocity of SNe Ia inferred from their  $z_{\text{hel}}$  and  $z_{\text{CMB}}$  values quoted by JLA, plotted versus the line-of-sight component of the velocity of the group the object belongs to in the CF3 dataset ( $\langle V_{\text{cmb}} \rangle - gp$ ). The horizontal bars are the diagonal errors in the JLA cosmology fit (statistical plus systematic), while the vertical bars indicate the random error of  $250 \text{ km s}^{-1}$  in the CF3 measurement. The green dashed line indicates when the two are equal, while the red dashed line shows the best-fit orthogonal distance regression which has a slope of 1.61, i.e. the JLA velocities have been underestimated on average by 48%. (Note that the outlier (SN1992bh) has a peculiar velocity of  $\sim 1000 \text{ km s}^{-1}$  according to JLA, but zero according to the CF3.)

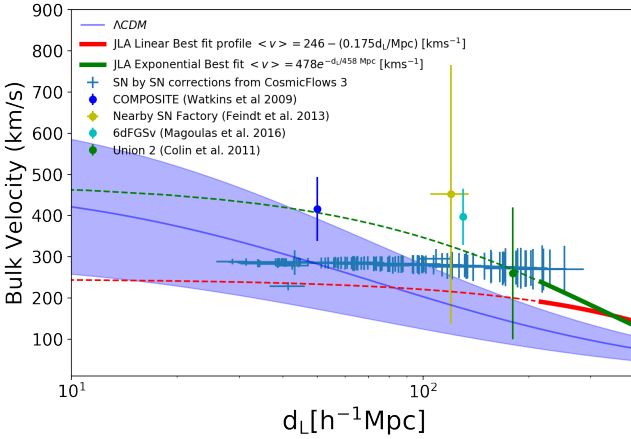


**Fig. 4.** The profile of bulk flow expected in a  $\Lambda$ CDM Universe using a top-hat window function is shown as the solid blue line, while the shaded region shows the  $\pm 1\sigma$  range. The red and green lines show, respectively, the linear and exponential fits to the bulk flow using JLA data (respectively rows (ix) and (x) of Table 1), along with the (blue) SN-by-SN corrections using CF3 data at smaller distances (the dashed lines indicate the extrapolated fits). Several measurements (with  $\pm 1\sigma$  uncertainties) using various surveys are shown for comparison.

by setting it to zero above  $d_L = P/Q'$  (see Fig. 4). The free parameters  $P$  and  $Q$  or  $Q'$  in our modelling of the bulk flow can be determined along with the usual 10 other free parameters used to fit the SNe Ia data.

The effect of an additional bulk flow term in the likelihood is to modify the distance modulus of eq.(A.1) such that:

$$\Delta m^{\text{bulk}}(P, Q, z_i) = - \left( \frac{5}{\ln 10} \right) \frac{(1 + z_i)^2}{H(z_i) d_L(z_i)} \hat{n}_i [P e^{-d_L(z_i)/Q}], \quad (7)$$

for the exponentially falling bulk flow, and likewise for the linearly falling bulk flow with the expression from eq.(6) substituted in the square brackets).

## 5. The likelihood analysis

We can rewrite both  $z_{\text{SN}}$  and  $z$  of eq.(1) as functions of the observed  $z_{\text{hel}}$ ,  $P$  and  $Q$  or  $Q'$  for the exponential (eq.5) or linear (eq.6) bulk flow models respectively. The Maximum Likelihood Estimator of Nielsen et al. (2016) is then used with the two additional parameters  $P$  and  $Q$  (or  $Q'$ ) for the bulk flow, in addition to the usual lightcurve fitting parameters in the SALT2 template (Betoule et al. 2014):  $\alpha, x_{1,0}, \sigma_{x_{1,0}}, \beta, c_0, \sigma_{c_0}, M_0, \sigma_{M_0}$ . Along with the two  $\Lambda$ CDM model parameters  $\Omega_m$  and  $\Omega_\Lambda$  we then have 12 parameters in total. As shown in Table 1, the following fits are performed (including an additional dispersion of  $c\sigma_z = 150 \text{ km s}^{-1}$  as recommended by Betoule et al. (2014)):

1. The same 10-parameter fit as in Nielsen et al. (2016), using only the  $z_{\text{CMB}}$  values provided by JLA.
2. The 10-parameter fit using  $d_L(z_{\text{CMB}}, z_{\text{hel}}) = [(1 + z_{\text{hel}})/(1 + z_{\text{CMB}})] d_L(z_{\text{CMB}})$  — as used by Davis et al. (2011) — and the JLA provided  $z_{\text{hel}}$  and  $z_{\text{CMB}}$  values.
3. 10-parameter fit as in (i), using only  $z_{\text{hel}}$  values (JLA provided) as was done in supernova analyses until 2011.
4. 10-parameter fit as in (i), using JLA provided  $z_{\text{hel}}$  values, after subtracting out bias corrections to  $m_B^*$ .
5. Exponentially falling bulk flow: 12-parameter fit (including the  $P$  and  $Q$  parameters of eq.(5), using only JLA provided  $z_{\text{hel}}$  values. No peculiar velocity corrections are applied.
6. Linearly falling bulk flow: 12-parameter fit (including the  $P$  and  $Q$  parameters of eq.(6) using only JLA provided  $z_{\text{hel}}$  values. No peculiar velocity corrections are applied.
7. JLA corrected redshifts + Exponential bulk flow: 12-parameter fit: SNe with peculiar velocity corrections applied by JLA, are treated as in (ii) above, while an exponentially falling bulk flow is fitted to the remaining SNe.
8. JLA corrected redshifts + Linear bulk flow: As in (vii), but with the linear parametrisation of the bulk flow.
9. CF-3 data & the Exponential bulk flow fit: 12-parameter fit using eq.(2) with the CF3-derived values of  $z_{\text{hel}}$  and  $z_{\text{CMB}}$  (see § 3) used for the low  $z$  SNe Ia to which the velocity correction can be applied. For the remaining objects, we use the JLA  $z_{\text{hel}}$  values, and an Exponential bulk flow is fitted using eq.(5) as described above.
10. CF-3 data & the Linear bulk flow fit: 12-parameter fit using eq.(6) with the CF3-derived values of  $z_{\text{hel}}$  and  $z_{\text{CMB}}$  (see § 3) used for the low  $z$  SNe Ia to which the velocity correction can be applied. For the remaining objects, we use the JLA  $z_{\text{hel}}$  values, and a Linear bulk flow is fitted using eq.(6).

In all above fits, the direction of the bulk flow is fixed to be that of the CMB dipole direction. This is reasonable as most of the previous analyses have shown large dipoles at intermediate redshifts converging to this direction (Watkins et al. 2009; Lavaux et al. 2010; Colin et al. 2011, 2017; Rameez et al. 2018). In Table 1 we also show the results for each fit after imposing the additional constraint of zero acceleration (‘No acceleration’) for a  $\Lambda$ CDM Universe i.e.:  $q_0 \equiv \Omega_\Lambda/2 - \Omega_m = 0$ . For the last 2 fits we show in addition the results after imposing the constraint of zero curvature (‘Flat’) for a  $\Lambda$ CDM Universe: i.e.  $\Omega_\Lambda + \Omega_m = 1$ .

The bulk flow can be fitted as  $478 \exp[-d_L/458 \text{ Mpc}] \text{ km s}^{-1}$  for the exponential decay form (eq.5), and  $[246 - 0.175(d_L/\text{Mpc})] \text{ km s}^{-1}$  for the linearly falling form (eq.6). Including the bulk flow *always* improves the quality of the fit as can be seen from the smaller values of  $-2 \log \mathcal{L}_{\text{max}}$ . This justifies the two additional parameters characterising it from an information-theoretic point of view. In all the above fits, apart from the ‘No acceleration’ ones, the best-fit bulk flow extends

beyond  $200h^{-1}$  Mpc with a velocity exceeding  $\sim 250 \text{ km s}^{-1}$ . Our results concerning the bulk flow are shown in Fig.4 along with selected recent observations.

Using the CF-3 data and the Linear bulk flow fit, as well as other fits of similar quality, the difference in the goodness of fit of the best model (with the lowest value of  $-2 \log \mathcal{L}_{\text{max}}$ ) w.r.t. the corresponding ‘No acceleration’ fit is now significantly smaller compared to previous studies. Fig. 5 clearly demonstrates the degeneracy between the derived value of  $\Omega_\Lambda$  and the local bulk flow, illustrating that the latter is an *essential* nuisance parameter to be added to cosmological fits when analysing SNe Ia. Allowing for the bulk flow in the fit demonstrates that the evidence for acceleration using SNe Ia data alone is even smaller than was found previously (Nielsen et al. 2016).

The results in Table 1 may be summarised as follows:

- Of all the fits, the only ones favouring  $\Omega_\Lambda > 0.5$  are just those which include the incorrect and incomplete peculiar velocity ‘corrections’ of JLA (Betoule et al. 2014).
- Fit (iv), which has *no* peculiar velocity corrections at all, as in Perlmutter et al. (1999) and Riess et al. (1998), prefers  $\Omega_\Lambda = 0.396$  with  $< 2\sigma$  evidence for acceleration.
- While previous work has suggested that bulk flows should not bias  $\Omega_\Lambda$ , it in fact drops by  $\sim 30\%$  if we undo the peculiar velocity ‘corrections’ of JLA and instead use the kinematic data from CF3. This illustrates the huge impact of considering a realistic LU-like observer such as ourselves, rather than the randomly located observer assumed in all previous analyses Hui & Greene (2006); Neill et al. (2007); Davis et al. (2011); Huterer et al. (2015). In particular this contradicts what is stated in Table 11 of Betoule et al. (2014).

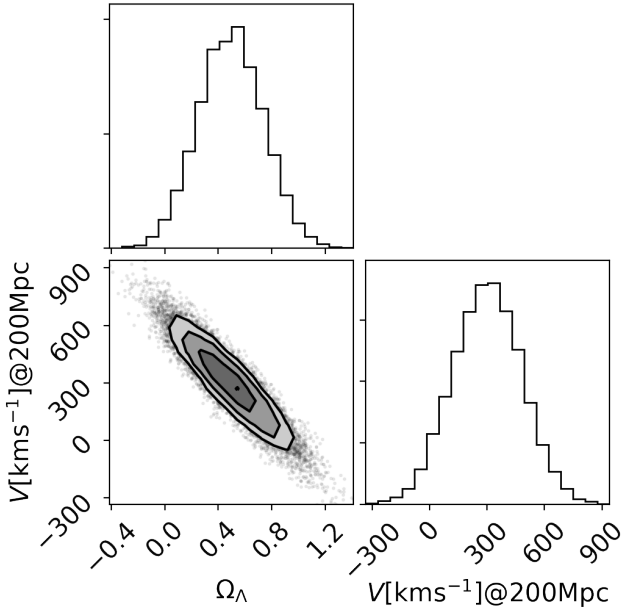


**Fig. 5.** 1, 2 and 3  $\sigma$  contours corresponding to the fit (ix) of Table 1 wherein peculiar velocities from CosmicFlows-3 are used for SN-by-SN corrections and the flow is allowed to continue beyond the extent of the survey with an exponential fall-off (eq.5). The velocity of the bulk flow at a top-hat smoothing scale of radius 200 Mpc is shown in the right histogram of the posterior, while the top histogram shows the extracted value of  $\Omega_\Lambda$ .

## 6. Discussion

Other authors have come to different conclusions regarding the impact of the bulk flow on cosmological parameter determination. Huterer et al. (2015) use, just as Hui & Greene (2006) did, the restricted longitudinal or conformal-Newtonian ‘gauge’ (see, Bertschinger 1993), to derive the covariance (eq.3) for a typical observer. But as shown in Fig.1 this would be relevant for observational cosmology only if each SNe Ia were being observed from a *different*, randomly sampled host galaxy. In practice we observe the real Universe from only one vantage point. Nevertheless Huterer et al. (2015) add this covariance as a “guaranteed theoretical signal” to the uncertainty budget of the JLA data, thus weakening the statistical preference for a bulk flow to  $\lesssim 2\sigma$  (as seen in their Fig.4). Huterer (2020) claims that any bias in the inference of dark energy parameters due to the effect of peculiar velocities can be determined *a priori* via simulations. This misses the point however that  $\Lambda$ CDM is a model and N-body simulations contain only as much physics as has been coded into them, i.e. neither necessarily capture the real Universe.

To summarise, we are *not* typical (‘Copernican’) observers — we are embedded in a fast and deep bulk flow and this has significant impact on the covariances used in supernova cosmology.<sup>1</sup> The usual procedure of adding a constant velocity dispersion of a few hundred  $\text{km s}^{-1}$  to account for peculiar velocities at high redshift, does not take into account the *correlated* flow of the galaxies. The JLA analysis (Betoule et al. 2014) corrected the data assuming the CMB dipole to be entirely kinematic in origin and further assumed that convergence to the CMB rest frame occurs abruptly at redshift  $z \sim 0.06$ . Since neither assumption is fully supported by observations, we have adopted a general model of the bulk flow which introduces two extra parameters in the analysis. This provides an independent estimate of the bulk flow and we find that it persists out to distances beyond  $200 h^{-1}$  Mpc, with a speed exceeding  $\sim 250 \text{ km s}^{-1}$ . Our maximum likelihood analysis then shows that the accelerated expansion of the Universe cannot be inferred as a statistically significant result from the SNe Ia data alone.

## References

- Bertschinger E., 1993, preprint ( arXiv:astro-ph/9503125)  
 Betoule M., Kessler R., Guy J., et al. 2014, A&A, 568, A22  
 Boggs P. T. & Rogers J. E., 1990, Contemp. Math., 112, 183  
 Carrick J., Turnbull S. J., Lavaux G. & Hudson M. J. 2015, MNRAS, 450, 317  
 Cautun M., Frenk C. S., van de Weygaert R., Hellwing W. A. & Jones B. J. T. 2014, MNRAS, 445, 2049  
 Colin J., Mohayaee R., Sarkar S. & Shafieloo A. 2011, MNRAS, 414, 264  
 Colin J., Mohayaee R., Rameez M. & Sarkar S. 2017, MNRAS, 471, 1045  
 Colin J., Mohayaee R., Rameez M. & Sarkar S. 2019a A&A, 631, L13  
 Colin J., Mohayaee R., Rameez M. & Sarkar S. 2019b preprint ( arXiv:1912.04257)  
 Conley A., Guy J., Sullivan M., et al. 2011, ApJS, 192, 1  
 Dam L. H., Heinesen A. & Wiltshire D. L. 2017 MNRAS, 472, 835  
 Davis T. M., Hui L., Frieman J. A., et al. 2011, ApJ, 741, 67  
 Desgrange C., Heinesen A. & Buchert T. 2019, Int. J. Mod. Phys. D, 28, 1950143  
 Feindt U., Kerschhaggl M., Kowalski M., et al. 2013, A&A, 560, A90  
 Guy J., Astier P., Baumont S., et al. 2007, A&A, 466, 11  
 Hellwing W. A., Bilicki M. & Libeskind N. I. 2018, Phys. Rev. D, 97, 103519  
 Hellwing W. A., Nusser A., Feix M. & Bilicki M. 2017, MNRAS, 467, 2787  
 Hong T., Springob C. M., Staveley-Smith L. et al. 2014, MNRAS, 445, 402-413  
 Hudson M. J., Smith R. J., Lucey J. R. & Branchini E. 2004, MNRAS, 352, 61  
 Hui L. & Greene P. B. 2006, Phys. Rev. D, 73, 123526  
 Hunt P. & Sarkar S. 2010, MNRAS, 401, 547  
 Huterer D., Shafer D. L. & Schmidt F. 2015, JCAP, 12, 033  
 Huterer D., 2020, ApJ, 904, L28

<sup>1</sup> There are other corrections too such as for gravitational lensing, which become more important than the effect of peculiar velocities at a redshift  $z > 0.15$  — see Figure B.1 of Colin et al. (2019a).

**Table 1.** Best-fit parameters and results for the fits described in § 5 using the Maximum Likelihood Estimator. Including the bulk flow improves the quality of the fit and decreases the significance of accelerated expansion, as seen from the decrease of  $-2 \log \mathcal{L}_{\max}$ .

	Fit	$-2 \log \mathcal{L}_{\max}$	$\Omega_m$	$\Omega_\Lambda$	$\alpha$	$x_{1,0}$	$\sigma_{x_{1,0}}$	$\beta$	$c_0$	$\sigma_{c_0}$	$M_0$	$\sigma_{M_0}$	$V \text{ (km s}^{-1}\text{)} @ 200h^{-1}\text{Mpc}$
(i)	Nielsen et al. (2016)	-214.97	0.341	0.569	0.134	0.0385	0.931	3.059	-0.016	0.071	-19.052	0.108	-
	No acceleration	-203.93	0.068	0.034	0.132	0.0327	0.932	3.045	-0.013	0.071	-19.006	0.110	-
(ii)	Nielsen et al. (2016) + JLA $z$	-221.93	0.340	0.565	0.133	0.0385	0.932	3.056	-0.016	0.071	-19.051	0.107	-
	No acceleration	-210.99	0.070	0.035	0.131	0.0328	0.932	3.042	-0.013	0.071	-19.006	0.109	-
(iii)	No pec. vel. corr. to $z$	-215.40	0.285	0.483	0.134	0.0398	0.932	3.038	-0.016	0.071	-19.051	0.108	-
	No acceleration	-207.67	0.051	0.025	0.132	0.0348	0.932	3.023	-0.014	0.071	-19.012	0.110	-
(iv)	No pec. vel. corr. to $z$ or $m_B$	-216.89	0.235	0.396	0.135	0.0397	0.932	3.029	-0.016	0.071	-19.040	0.109	-
	No acceleration	-211.84	0.0413	0.021	0.133	0.0357	0.932	3.016	-0.014	0.071	-19.008	0.110	-
(v)	Exponential bulk flow	-217.51	0.289	0.452	0.134	0.0390	0.932	3.036	-0.016	0.071	-19.037	0.107	253
	No acceleration	-211.3	0.077	0.039	0.132	0.0347	0.932	3.024	-0.014	0.071	-19.002	0.108	292
(vi)	Linear bulk flow	-217.47	0.290	0.455	0.134	0.0390	0.932	3.036	-0.016	0.071	-19.038	0.107	265
	No acceleration	-211.99	0.082	0.041	0.132	0.0347	0.932	3.025	-0.014	0.071	-19.002	0.108	282
(vii)	JLA + Exp. bulk flow	-224.87	0.340	0.570	0.133	0.0387	0.932	3.051	-0.016	0.072	-19.052	0.107	271
	No acceleration	-216.3	0.077	0.039	0.132	0.0347	0.932	3.024	-0.014	0.071	-19.002	0.108	295
(viii)	JLA + Lin. bulk flow	-225.08	0.341	0.577	0.133	0.0387	0.932	3.050	-0.016	0.071	-19.054	0.107	238
	No acceleration	-214.14	0.072	0.036	0.131	0.0328	0.932	3.041	-0.013	0.071	-19.005	0.109	251
(ix)	CF3 + Exp. Bulk Flow	-225.61	0.279	0.427	0.133	0.0386	0.932	3.001	-0.016	0.071	-19.034	0.109	309
	No acceleration	-220.72	0.086	0.043	0.132	0.0346	0.932	2.990	-0.015	0.071	-19.001	0.110	398
	Flat	-223.96	0.393	0.607	0.133	0.0357	0.933	2.998	-0.016	0.071	-19.045	0.110	338
(x)	CF3 + Lin. bulk flow	-225.73	0.277	0.431	0.133	0.0386	0.932	3.002	-0.016	0.071	-19.037	0.109	211
	No acceleration	-220.16	0.085	0.042	0.132	0.0346	0.932	2.991	-0.015	0.071	-19.001	0.110	249
	Flat	-224.18	0.390	0.610	0.134	0.0399	0.932	3.006	-0.016	0.071	-19.047	0.109	215

- Karpenka N. V. 2015, preprint (arXiv:1503.03844)  
Lavaux G., Tully R. B., Mohayaee R. & Colombi S., 2010, ApJ, 709, 483  
Leibundgut B. 2000, Astron. Astrophys. Rev., 10, 179  
Magoulas C., Springob C., Colless M., et al. 2016, Proc. IAU Symp., 308, 336  
March M., Trotta R., Berkes P., Starkman G. & Vaudrevange P. 2011, MNRAS, 418, 2308  
Mohayaee R., Rameez M. & Sarkar S. 2021 Eur. Phys. J. Spec. Top., 230, 2067  
Neill J. D., Hudson M. J. & Conley A. 2007, ApJ, 661, L123  
Nielsen J. T., Guffanti A. & Sarkar S. 2016, Sci. Rep., 6, 35596  
Nielsen J. T. 2015, preprint (arXiv:1508.07850)  
Perlmutter S., Aldering G., Goldhaber G. et al. 1999, ApJ, 517, 565  
Rameez M., Mohayaee R., Sarkar S. & Colin J. 2018, MNRAS, 477, 1772  
Rameez M. & Sarkar S. 2021 Class. Quantum Grav., 38, 154005  
Riess A. G., Filippenko A. V., Challis P. et al. 1998, AJ, 116, 1009  
Rubin D. & Hayden B. 2016, ApJ, 833, L30  
Saunders W., Sutherland W. J., Maddox S. J. et al. 2000, MNRAS, 317, 55  
Scolnic D.M., Jones, D.O., Rest, A. et al. 2018, ApJ, 859, 101  
Shariff H., Xiao J., Trotta R. & van Dyk D. A. 2016 ApJ, 827, 1  
Skillman S. W., Warren M. S., Turk M. J. et al. 2014, preprint (arXiv:1407.2600)  
Tully R. B., Courtois H. M. & Sorce J. G. 2016, AJ, 152, 50  
Watkins R., Feldman H. A. & Hudson M. J. 2009, MNRAS, 392, 743



## Appendix A: Supernova Cosmology

The largest public catalogues of SNe Ia lightcurves, the JLA (Betoule et al. 2014) and its successor Pantheon (Scolnic et al. 2017), employ the ‘Spectral Adaptive Lightcurve Template 2’ (SALT2) to fit each SNe Ia light curve with 4 parameters: the apparent magnitude  $m_B^*$  (at maximum in the rest frame ‘B-band’), the ‘shape’ and ‘colour’ corrections,  $x_1$  and  $c$  (Guy et al. 2007).<sup>2</sup>The distance modulus is then:

$$\mu_{\text{SN}} = m_B^* - M + \alpha x_1 - \beta c, \quad (\text{A.1})$$

where  $\alpha$  and  $\beta$  are assumed to be constants, as is  $M$  the absolute SNe Ia magnitude. In the standard  $\Lambda$ CDM cosmological model this is related to the luminosity distance  $d_L$  as:

$$\begin{aligned} \mu &\equiv 25 + 5 \log_{10}(d_L/\text{Mpc}), \quad \text{where:} \\ d_L &= (1+z) \frac{d_H}{\sqrt{\Omega_k}} \sin \left( \sqrt{\Omega_k} \int_0^z \frac{H_0 dz'}{H(z')} \right), \text{ for } \Omega_k > 0 \\ &= (1+z) d_H \int_0^z \frac{H_0 dz'}{H(z')}, \text{ for } \Omega_k = 0 \\ &= (1+z) \frac{d_H}{\sqrt{\Omega_k}} \sinh \left( \sqrt{\Omega_k} \int_0^z \frac{H_0 dz'}{H(z')} \right), \text{ for } \Omega_k < 0 \\ d_H &= c/H_0 \approx 3000 h^{-1} \text{ Mpc}, \quad H_0 \equiv 100 h \text{ km s}^{-1} \text{ Mpc}^{-1}, \\ H &= H_0 \sqrt{\Omega_m(1+z)^3 + \Omega_k(1+z)^2 + \Omega_\Lambda}. \end{aligned} \quad (\text{A.2})$$

Here  $H$  the Hubble parameter ( $H_0$  being its present value),  $d_H$  is the ‘Hubble distance’ and  $\Omega_m, \Omega_\Lambda, \Omega_k$  are the matter, cosmological constant and curvature densities in units of the critical density. In the standard  $\Lambda$ CDM model these are related by the ‘cosmic sum rule’:  $1 = \Omega_m + \Omega_\Lambda + \Omega_k$ , which is simply rewriting the Friedmann equation.

Thus knowing the redshift and distance of the ‘standardised’ SNe Ia, one can determine the cosmological parameters. However these are measured from Earth and usually quoted in the heliocentric frame (allowing for the Earth’s motion around the Sun), so need to first be translated to the reference frame in which the universe is (statistically) isotropic and homogeneous and the above equations hold. Assuming that the CMB dipole is purely kinematic in origin, this is taken to be the ‘CMB frame’ which can be reached by a local special relativistic boost, so the measured values are corrected as in eq.(1) for the redshift and eq.(2) for the luminosity distance.

## Appendix B: The Joint Lightcurve Analysis catalogue

The JLA catalogue (Betoule et al. 2014) consists of 740 spectroscopically confirmed SNe Ia, including several low redshift ( $z < 0.1$ ) samples, three seasons of SDSS-II ( $0.05 < z < 0.4$ ) and three years of SNLS ( $0.2 < z < 1$ ) data, all calibrated consistently in the ‘Spectral Adaptive Lightcurve Template 2’ (SALT2) scheme. Figs. B.1 and B.2 show respectively the sky coverage and redshift distribution of this publicly available catalogue.

We use the publicly available SALT2 light curve fits done by the JLA collaboration (Betoule et al. 2014) but rather than their ‘constrained’  $\chi^2$  statistic which is unprincipled, we employ the Maximum Likelihood Estimator of Nielsen et al. (2016). Our

<sup>2</sup> The SALT2 template also allows for a ‘host galaxy mass correction’ to be included in eq.(A.1), however Nielsen (2015) found that the Maximum Likelihood Estimator is insensitive to this parameter.

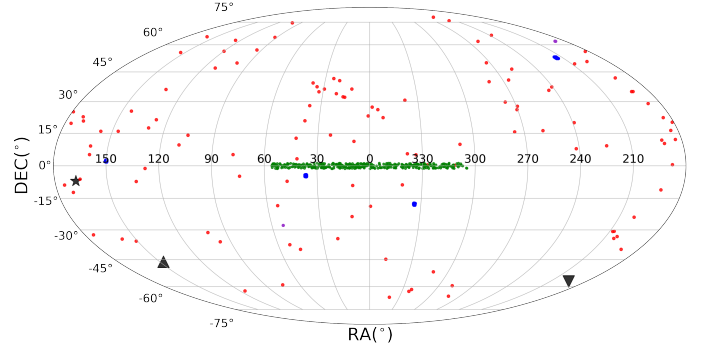


**Fig. B.1.** Sky distribution (Mollweide projection, equatorial coordinates) of the 4 subsamples of the JLA catalogue: low  $z$  (red dots), SDSS (green dots), HST (black dots), clusters of many SNe Ia from SNLS (blue dots). The directions of the CMB dipole (star), the SMAC bulk flow (triangle) (Neill et al. 2007), and the 2M++ bulk flow (inverted triangle) (Carrick et al. 2015) are shown in grey.

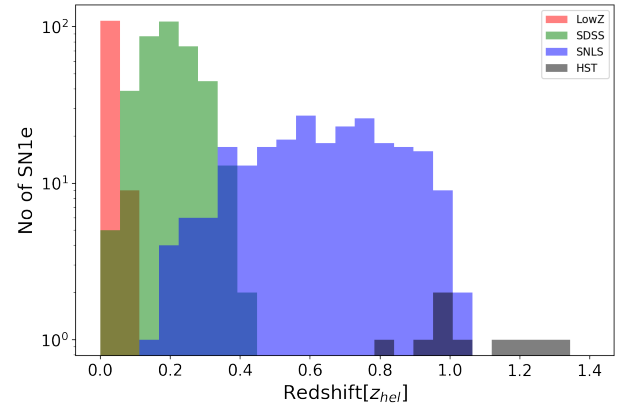


**Fig. B.2.** The redshift distribution of the 4 samples that make up the SDSS-II/SNLS3 Joint Lightcurve Analysis catalogue.

approach, is frequentist but equivalent to the ‘Bayesian Hierarchical Model’ (March et al. 2011; Shariff et al. 2015; Rubin & Hayden 2016). It has been used in independent analyses of SNe Ia by Dam, Heinesen & Wiltshire (2017) and Desgrange et al. (2019).

Rubin & Hayden (2016) have advocated that the shape and colour parameters be allowed to depend on both the SNe Ia sample and the redshift, however this introduces 12 additional parameters (to the 10 used above) and thus violates the Bayesian information criterion (Colin et al. 2019a,b). Karpenka (2015) noted that if  $x_1$  and  $c$  evolve with redshift, the likelihood-based methods return biased values of the parameters (while the ‘constrained  $\chi^2$ ’ method continues to be robust), however this conclusion is arrived at using Monte Carlo simulations which *assume* the  $\Lambda$ CDM model and is therefore a circular argument. It has been emphasised by Dam, Heinesen & Wiltshire (2017) that systematic uncertainties and selection biases in the data need to be corrected for in a model-independent manner, *before* fitting to a particular cosmological model. For further discussion of these (and related) issues see Mohayaee et al. (2021).